Stability enhancement of polymer electrolyte membrane fuel cells based on a sulfonated poly(ether ether ketone)/poly(vinylidene fluoride) composite membrane

Kyung A Sung, Wan-Keun Kim, Keun-Hwan Oh, Min-Ju Choo, Kwan-Woo Nam, Jung-Ki Park*

Department of Chemical and Biomolecular Engineering, Korea Advanced Institute of Science and Technology, 373-1, Guseong-Dong, Yuseong-Gu, Daejeon 305-701, Republic of Korea

ABSTRACT

Most proton-conducting membranes based on sulfonated aromatic polymers exhibit significant dimensional change by hydration, and this leads to degradation of fuel cell performance on prolonged operation. In this study, as a means of improving the stability of a polymer electrolyte membrane fuel cell, composite membranes employing a porous poly(vinylidene fluoride) (PVdF) substrate and sulfonated poly(ether ether ketone) (sPEEK) electrolyte are prepared and their hydration behaviours, including water uptake and dimensional change, are examined. The electrochemical characteristics of membrane/electrode assemblies using the sPEEK/PVdF composite membrane are also analyzed. The initial cell performance is comparable with that of a cell based on a pure sPEEK membrane. Furthermore, the stability of the cell using the sPEEK/PVdF composite membrane is considerably improved during a humidity cycle test wherein hydration and dehydration are periodically repeated.

1. Introduction

Polymer electrolyte membrane fuel cells (PEMFCs) have been developed to produce efficient and environmentally friendly energy for stationary, transportation, and portable applications [1]. In the PEMFC, a proton-conducting polymer is employed as the membrane. Perfluorinated sulfonic acid-based ionomers, such as Nafion® produced by Du Pont, are the most widely used membranes due to their high proton conductivity, high chemical/electrochemical stability, and good mechanical strength [2]. It is generally understood, however, that a Nafion membrane has several critical drawbacks, such as high cost, high fuel permeability, and limited operational temperature. In seeking substitutes for Nafion membranes, numerous alternative membranes have been proposed and most are sulfonated aromatic polymer membranes, e.g., including sulfonated poly(arylene ether sulfone), sulfonated poly(ether ether ketone) (sPEEK), sulfonated polyimide [3–5]. In general, these alternative membranes are designed to have a large number of sulfonic acid groups so as to obtain high proton conductivity, and thus high ion exchange capacity (IEC). High IEC derived from a high concentration of acid groups results in substantial water uptake, and such membranes exhibit poor

dimensional stability due to polymer expansion by hydration [6]. Upon humidity cycling during cell operation, the membrane undergoes dimensional changes, while a relatively rigid electrode tends to maintain its original dimensions. Even if the membrane and the electrode are initially well bonded, the difference in hydration behaviour can cause mechanical stress between these two components. Sulfonated aromatic polymer membranes including a sPEEK membrane, exhibit higher water uptake than Nafion and thus the dimensional change of the membrane–electrode assembly (MEA) based on sulfonated aromatic polymer membranes becomes much more significant. This causes an apparent edge failure between the membrane and the electrode after long-term operation of a PEMFC that is likely one of the main reasons for poorer cell durability [7].

To minimize the dimensional change of the membrane, there have been several attempts to prepare composite membranes that comprise a porous substrate and a polymer electrolyte which fills the porous substrate [8]. The composite membrane can achieve high dimensional stability because the introduction of a porous substrate suppresses membrane swelling by hydration. To this end, most work in this regard has concentrated on the properties of the membrane itself or on the initial cell performance behaviour [9–11]. Although there have been a few reports that fuel cells with composite membranes employing a porous substrate show good stability for a certain period of time [12,13], a clear explanation of the influence of the dimensional stability of the membrane on cell durability has yet to be offered.

* Corresponding author. Tel.: +82 42 350 3965; fax: +82 42 350 3910.
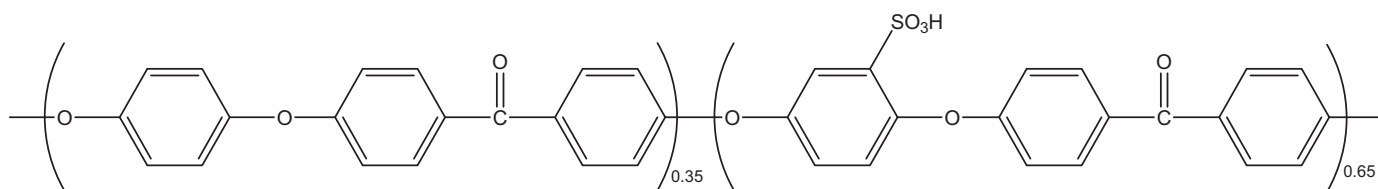 E-mail address: jungpark@kaist.ac.kr (J.-K. Park).

Fig. 1. Molecular structure of sPEEK (DS 65%).

To evaluate the effect of membrane stability on the cell durability, this study compares the performance of a fuel cell based on a composite membrane with that based on a pure sPEEK membrane. Given that the dimensional change of the membrane is usually very sensitive to humidity, the change in cell performance with humidity cycling is examined.

2. Experimental

2.1. Preparation of porous PVdF substrate and morphological analysis

Porous substrates were prepared using PVdF (SOLEF6020, Solvay Solexis) and diphenyl phthalate (DPhP) as materials for the matrix and the pore former, respectively. First, 10 wt.% solutions of PVdF and DPhP in N,N-dimethylacetamide (DMAc) were prepared independently, and then mixed with different ratios to provide porous substrates that had a range of porosities. The mixtures were then cast on a glass plate using a doctor blade to control the thickness of the porous substrate. The cast mixtures were dried at 70 °C for 24 h, and subsequently at 100 °C for a following 24 h. After drying, they were impregnated with methanol to extract DPhP and repeatedly washed for complete extraction of DPhP to produce a porous PVdF substrate. A porous substrate fabricated with greater than 70 wt.% of DPhP could not yield a self-standing film and thus porous PVdF substrates made with less than 60 wt.% of DPhP are used in this study.

To analyze the pore structure of the PVdF substrate, the porosity was measured by mercury porosimetry (Autopore IV 9500, Micrometrics). Both surface and cross-sectional images were also obtained by means of scanning electron microscopy (SEM) (Sirion, FEI).

2.2. Preparation of sPEEK/PVdF composite membranes

sPEEK was prepared by sulfonation of poly(ether ether ketone) (Aldrich) according to a procedure reported elsewhere [14,15]. The degree of sulfonation of the resulting polymer was 65% and its molecular structure is shown in Fig. 1. Before filling the pores with sPEEK solution, sPEEK was swollen in deionized water at 80 °C and 1-propanol was subsequently added under stirring and continuous heating.

For filling the polymer electrolyte into the porous substrate, the sPEEK solution was poured on the surface of the porous PVdF substrate to extend over the glass plate and impregnated the empty pores of the substrate by the force of gravity. After drying in an oven at 70 °C for 24 h, the film was reversed and the sPEEK solution was again poured on the surface of the substrate. The same drying process as described above was repeated. After four repeated filling and drying processes, a sPEEK/PVdF composite membrane was eventually obtained. The composite membrane was fully protonated using a 1.0 M sulfuric acid solution at room temperature for 24 h, followed by thorough rinsing with deionized water. To ensure complete filling of the sPEEK electrolyte into the porous PVdF substrate, a cross-sectional SEM image of the sPEEK/PVdF composite membrane was examined. For comparison, a pure sPEEK membrane was

also prepared by a solution casting method. The sPEEK solution (10 wt.%) in N-methyl-2-pyrrolidone (NMP) was directly cast on a clean glass plate, and dried at 70 °C for 24 h and subsequently under vacuum at 120 °C for the following 24 h. The protonation process of the sPEEK membrane was the same as that applied for the sPEEK/PVdF composite membrane.

2.3. Characterization of sPEEK/PVdF composite membrane

To investigate the change in mechanical properties by hydration, the tensile strength of the pure sPEEK membrane and the sPEEK/PVdF composite membrane was measured in both dry and hydrated states using a universal testing machine (INSTRON 5583). To attain a hydrated state, membranes were immersed in deionized water at room temperature for 24 h and their tensile strength was measured immediately after removal from the water bath.

Water uptake and dimensional change were also measured by the differences in weight and dimensions between the dry and the wet membranes. The wet membrane, after soaking in deionized water at 65 °C for 1 h, was wiped and its weight, length and thickness were measured immediately. The dry membrane was obtained by vacuum drying at 120 °C for at least 24 h. The water uptake and the dimensional change Δl (or Δt) of the membranes were calculated as follows:

$$\text{Water uptake } (\%) = \frac{W_{\text{wet}} - W_{\text{dry}}}{W_{\text{dry}}} \times 100 \tag{1}$$

$$\Delta l \text{ (or } \Delta t) = \frac{l_{\text{wet}} - l_{\text{dry}}}{l_{\text{dry}}} \left(\text{or } \frac{t_{\text{wet}} - t_{\text{dry}}}{t_{\text{dry}}} \right) \times 100 \tag{2}$$

where W_{wet}, l_{wet}, and t_{wet} are the weight, length and thickness of the wet membrane, respectively, and W_{dry}, l_{dry}, and t_{dry} are the corresponding values for the dry membrane.

The through-plane ion conductivities of sPEEK/PVdF composite membranes in deionized water at 65 °C were determined by mean of a.c. impedance spectroscopy measurements (1400 FRA and 1470E, Solartron) over a frequency range from 10^6 to 1 Hz. As shown in Fig. 2(a), the membrane was held between two carbon papers (TGPH090, Toray) connecting copper foil and were mounted on polytetrafluoroethylene (PTFE) moulds with an open window. The conductivity cell was clamped tightly by four bolts and nuts. For through-plane conductivity measurements, the electrode must have the ability to pass water as well as the ability to conduct electrons, and therefore carbon paper with a high porosity, 78%, was employed. A photograph of the conductivity cell after assembling the membrane, carbon papers and PTFE moulds is given in Fig. 2(b). To eliminate the interfacial resistance between the membrane and the electrode, the resistance of membranes with different thicknesses was examined and the through-plane conductivity was calculated on the basis of the difference in resistance between two membranes with different thicknesses.

2.4. Fabrication of MEAs and single cell test

To fabricate MEAs for the cell test, the sPEEK/PVdF composite membranes were sandwiched between two gas-diffusion elec-
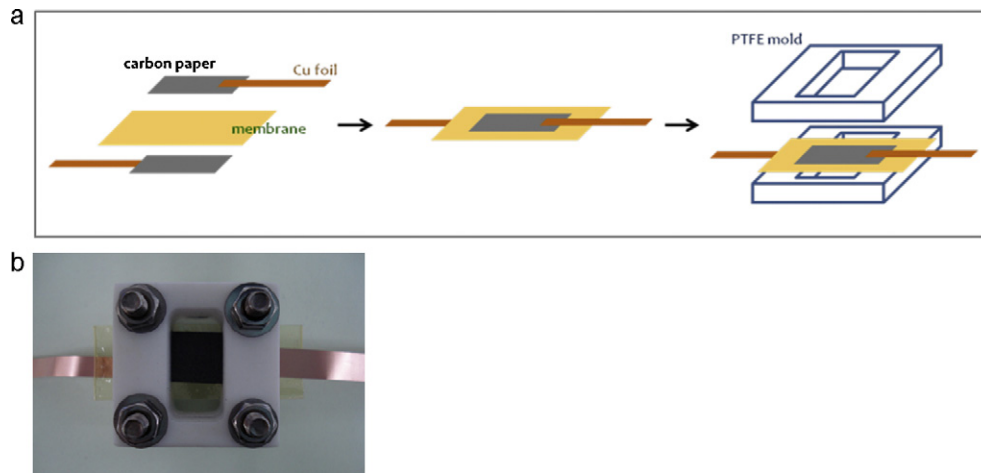
Fig. 2. (a) Schematic illustration of preparation process for through-plane conductivity measurements and (b) photographic image of a conductivity cell.

trodes (LT 140E-W, ETEK) by hot-pressing at 130 °C for 5 min under 1500 psi. The gas-diffusion electrode was composed of a hydrophobic gas-diffusion layer and an electrocatalyst layer incorporating an ionomer. The geometric electrode area was 25 cm² and Pt loading was 0.5 mg cm⁻² on both the anode and the cathode.

For current–voltage polarization, MEAs were connected to a test station equipped with an electronic load (SMART II, Won-A Tech, Korea). The anode was fed with humidified hydrogen gas at a flow rate of 500 cm³ s⁻¹ and the cathode was fed with air at a flow rate of 1500 cm³ s⁻¹ without back-pressure. For the 100% RH condition, the humidifier temperature was set to 65 °C, i.e., the same as the cell temperature, and the temperature of the gas inlet-line was maintained at 70–75 °C to prevent the condensation of the humidified gas into liquid water. After sufficient humidification, the current–voltage curve of each MEA was obtained at 65 °C and, to analyze the voltage loss with the current, impedance measurements were also performed. The frequency range was from 10^4 to 10^{-1} Hz and the impedance spectra were reported at 0.6 V of the cell potential.

2.5. Humidity cycle tests

After initial evaluation of the performance of the PEMFC, humidity cycling tests were conducted to examine the effect of the porous substrate on cell performance under such conditions. For this experiment, non-humidified and fully humidified nitrogen gas at a flow rate of 1000 cm³ s⁻¹ was supplied in turn every 30 min. During the dehydration process, the gas line was not connected with the humidifier, whereas fully humidified gas was supplied from the humidifier during the hydration process. Current–voltage curves were taken every 10 humidity cycles.

3. Results and discussion

3.1. Preparation of porous PVdF substrates

Among the several methods available to prepare a porous substrate, the method of phase-inversion induced by a non-solvent has been widely used due to its simplicity. During this process, a polymer-rich phase forms a solid substrate while a polymer-poor phase generates liquid-filled pores [16,17]. In general, morphology control of the porous substrate is rather complicated, as it is dependent on the exchange rate as well as the compatibility between the solvent and non-solvent [18,19]. In addition, porous substrates originating from phase-inversion exhibit a significant imbalance of pore structure: a circle-type pore is formed in the top layer

whereas a sponge- or finger-type pore is formed in the sub-layer of the substrate. Thus, in this experiment, porous PVdF substrates were prepared by extraction of a pore former, DPhP, rather than by phase-inversion. In addition to its simplicity, another advantage of the preparation method using a pore former is the formation of a homogeneous pore structure that endows the composite membrane with uniform characteristics over the whole membrane. The resulting pore structure created with a pore former is shown in Fig. 3. According to surface and cross-sectional SEM images of the porous substrate, an isotropic pore structure is formed in both the in-plane and the through-plane directions. The thickness of the
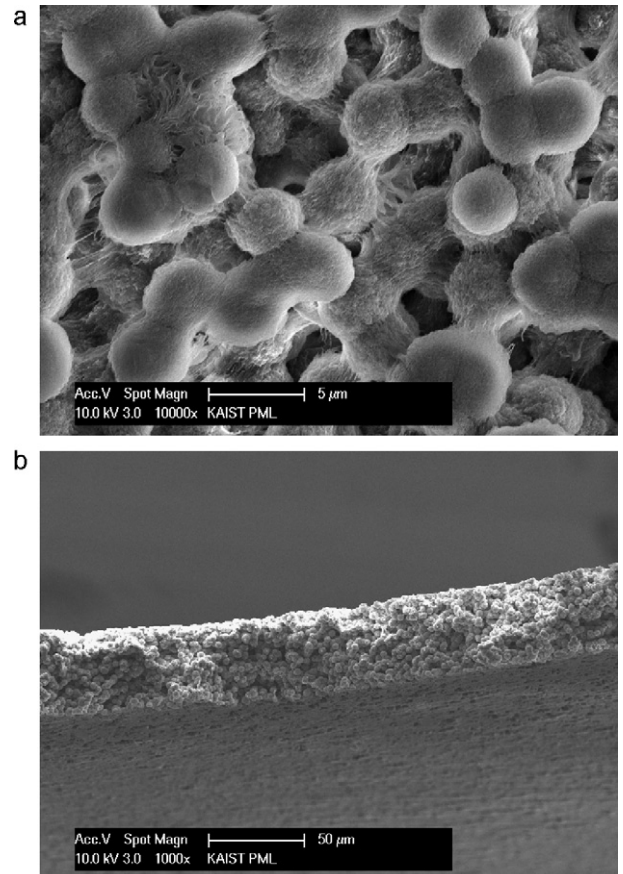
Fig. 3. SEM images of (a) surface and (b) cross-section of porous PVdF substrates.

Table 1
Porosity of three different porous PVdF substrates: XX in label "P-XX" denotes weight percent (wt.%) of pore former in mixture of PVdF and DPhP.

P-XX	PVdF:DPhP (wt.%)	Porosity (%)
P-40	60:40	60.5
P-50	50:50	68.4
P-60	40:60	76.0

Table 2
Mechanical strength of several membranes in dry and hydrated states.

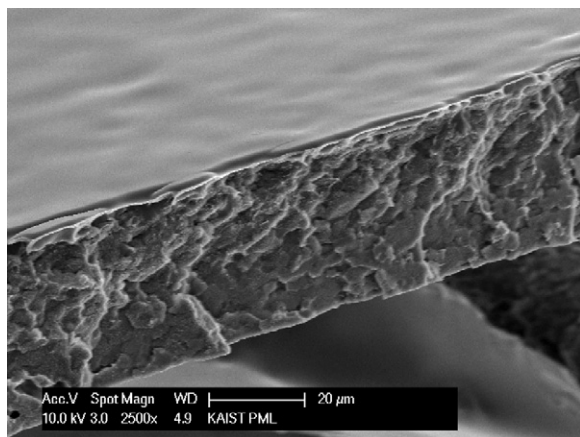|	Tensile strength (MPa)	
	Dry state	Hydrated state
cP-40	58.3	29.5
cP-50	53.7	25.6
cP-60	53.1	25.0
Nafion 112	26.3	20.5
sPEEK	44.2	9.0

porous substrate was controlled by the thickness of the doctor blade, and porous PVdF substrates with roughly 20–40 μm thickness were used to fabricate MEAs.

The porosity of the PVdF substrate was evaluated by mercury porosimetry and was shown to increase with the content of pore former. Since a substrate with low porosity could not accommodate a sufficient amount of sPEEK electrolyte for proton conduction, PVdF substrates with a porosity higher than 50% were chosen in this study. In addition, as described previously, with greater than 70 wt.% pore former a self-standing substrate could not be fabricated, and thus three different appropriate porous PVdF substrates were selected, as listed in Table 1. In the list, XX denotes the weight percent (wt.%) of the pore former in the mixture of PVdF and DPhP.

3.2. Preparation of sPEEK/PVdF composite membrane

For the sPEEK/PVdF composite membrane, sPEEK was impregnated into a porous PVdF substrate. Since several effective solvents for sPEEK, such as NMP, *N,N*-dimethylformamide and DMAc, can also dissolve PVdF, they were not used as solvents or the electrolyte solution. It is well known that PVdF has good wettability with alcohol and thus an alcohol/water mixture was used as a solvent for the electrolyte solution. Although sPEEK cannot dissolve in pure alcohol, its solubility is reported to improve significantly after swelling in water [20].

After filling the electrolyte into the substrate, an SEM image of the sPEEK/PVdF composite membrane was taken to evaluate whether the sPEEK electrolyte completely filled the pores of the substrate. It was ascertained that four repeats of the electrolyte filling process was sufficient for complete filling of the electrolyte. A cross-sectional SEM image of the composite membrane after carrying out the filling procedure four times is presented in Fig. 4. The image reveals that the pores of the PVdF substrate are well-filled with sPEEK electrolyte. The resulting composite membranes were labeled "cP-XX", which designates a composite membrane using a porous substrate P-XX.

Fig. 4. Cross-sectional SEM image of sPEEK/PVdF composite membrane after injection of electrolyte.

3.3. Effect of porous substrate on membrane properties

The mechanical strength of the sPEEK/PVdF composite membranes, Nafion 112, and the pure sPEEK membrane, in both dry and hydrated states, is listed in Table 2. Since the porous PVdF substrate acts as a mechanical support, the tensile strength of the composite membranes is higher than that of Nafion 112 and the pure sPEEK membrane, respectively, and the improvement is especially noticeable in the hydrated state. It is well known that, because water in the membrane can act as a plasticizer, a hydrated membrane possesses lower mechanical strength than a dry membrane; accordingly, the mechanical strength of all the membranes studied in this work decreases after hydration. In comparison with the pure sPEEK membrane, however, the loss of mechanical strength with hydration is considerably reduced for the sPEEK/PVdF composite membrane. This is because the high hydrophobicity of PVdF effectively prevents the composite membrane from absorbing water and thereby the effect of water as a plasticizer becomes less significant. In other words, the relatively high tensile strength of the sPEEK/PVdF composite membrane in the hydrated state results from a combination of the hydrophobicity of PVdF itself and the effect of the porous substrate as a mechanical support.

To investigate the effect of porous PVdF substrates on membrane swelling, the water uptake and the dimensional change of the sPEEK/PVdF composite membrane were measured; the results are summarized in Table 3. The water uptake was based on the weight of both the sPEEK/PVdF composite membrane and only sPEEK in the composite membrane. Although the former increases slightly with the content of pore former and the latter is similar irrespective of the porous substrate, both values are much lower than those of the pure sPEEK membrane. In addition, the dimensional stability of the composite membrane increases remarkably compared with that of the pure sPEEK membrane. This is because the high hydrophobicity of PVdF and the good mechanical strength of the porous PVdF substrate enhance the dimensional stability of the composite membrane.

To evaluate the ability to conduct protons, through-plane proton conductivities of the sPEEK/PVdF composite membrane were measured in deionized water at 65 °C. In the measurement of

Table 3
Water uptake, dimensional stability, and through-plane conductivities of several membranes: prefix c in label "cP-XX" denotes composite membrane using porous substrate P-XX.

	Water uptake (wt.%)	Dimensional change (%)			Proton conductivity (S cm^{-1})
		Δl	Δt	Δv	
cP-40	20[a]/42[b]	5	8	19	0.018
cP-50	24[a]/43[b]	7	11	27	0.022
cP-60	27[a]/41[b]	7	12	28	0.024
Nafion 112	40	18	18	64	0.040
sPEEK	88	28	25	105	0.036

[a] Water uptake based on weight of dry sPEEK/PVdF composite membrane.
[b] Water uptake based on weight of sPEEK in dry sPEEK/PVdF composite membrane.

through-plane conductivities, there are several factors that should be considered including the electrode resistance and the interfacial resistance between the electrode and membrane [21]. To eliminate the effects of these factors on proton conductivities, the resistances of membranes with different thicknesses were measured and their differences were calculated. In the evaluation of proton conductivity, the values of differences in the resistance and in the membrane thickness were employed instead of the direct values of the resistance and the membrane thickness. The through-plane conductivities of the composite membrane, the pure sPEEK membrane and Nafion membrane are shown in Table 3. For through-plane conductivity measurements of the Nafion membranes, Nafion 112 membrane with 51 μm and Nafion 115 membrane with 127 μm were used. As shown in Table 3, although the proton conductivities of the sPEEK/PVdF composite membranes increase with the pore former content, they are lower than those of the Nafion and pure sPEEK membranes, respectively. Since the porous substrate has no ionic groups such as with sulfonic acid, the number of proton sources for the composite membrane is smaller than that for the pure sPEEK membrane, and therefore the proton conductivity is somewhat sacrificed. The ability of the porous substrate to provide mechanical support, however, makes it possible to form a thinner composite membrane which, in turn, can provide a shorter pathway for proton conduction. The loss of proton conductivity caused by the reduction in the number of proton sources could thus be compensated using a thin composite membrane.

The through-plane conductivities of the pure sPEEK membrane, which is known to be an isotropic membrane [21], are around only 30% of the in-plane conductivities, as reported in a previous study [22]. It appears that the hydrophobic property of carbon paper hinders hydration of the membrane for through-plane proton conduction, even though carbon paper has a higher porosity and also the PTFE mould has an open window providing exposure to water.

3.4. Effect of porous substrate on initial cell performance

To investigate the effect of the porous substrate on initial cell performance, several MEAs were fabricated using the sPEEK/PVdF composite membrane, a pure sPEEK membrane, and a Nafion 112 membrane. Two composite membranes with different thicknesses were employed to fabricate MEAs and the thickness of the first membrane was 40 μm, corresponding with that of the pure sPEEK membrane. The other membrane had a thickness of 22 μm, which was selected to evaluate the effect of membrane thickness on cell performance. For these two composite membranes, the same porous substrate, P-60, was used, as this membrane showed relatively high proton conductivity compared with the other composite membranes. The cell was operated at 65 °C and the humidifier temperature of both the fuel and the oxidant was also 65 °C. As shown in Fig. 5, the cell based on a cP-60 membrane with 40 μm thickness gives much poorer performance than cells based on Nafion 112 or a pure sPEEK membrane, and this appears to be due to the lower proton conductivity of the cP-60 membrane. For the thinner cP-60 membrane (22 μm), however, the cell performance is much better; this implies that the lower thickness of the composite membrane can compensate for the poorer conductivity of the composite membrane in the overall performance of the cell.

Fig. 6 shows the impedance spectra at 0.6 V, at which there are two intersections with the real axis of the applied frequency. The smaller one obtained at high frequency is related to the ohmic resistance and the interval between two intersections represents the charge-transfer resistance by the electrochemical reaction at the electrode [23]. As shown in Fig. 6, the charge-transfer resistance is similar irrespective of the type of membranes employed in each MEA, because the electrode reactivity would be similar when using the same electrode in the MEAs. By contrast, whereas the
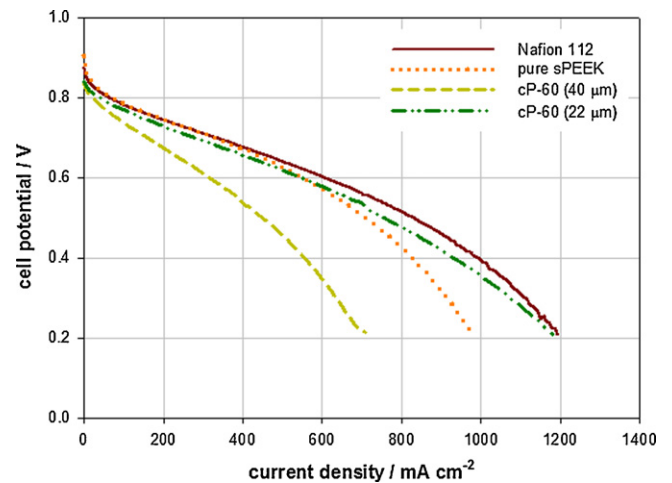

Fig. 5. Initial cell performance of four different MEAs at 65 °C: humidified H_2 gas and air supplied to anode and cathode, respectively.
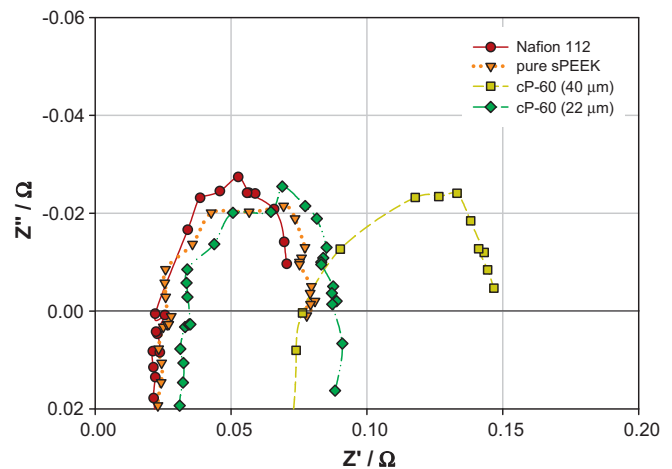

Fig. 6. Impedance spectra of four different MEAs during cell operation at a d.c. potential of 0.6 V.

thick cP-60 membrane has a large ohmic resistance, the thin cP-60 membrane has an ohmic resistance similar to that of the Nafion 112 and pure sPEEK membranes. The ohmic resistance is related to the flow of electrons through the electrode and the various interconnections as well as the flow of protons through the membrane [24]. As all MEAs were assembled using the same components except for the membrane in this experiment, the difference in the membrane resistance can be regarded as the main reason for the difference of ohmic resistance. It is thus concluded that the reduced ohmic resistance of the thin composite membrane is due to a shorter proton pathway compared with the thick composite membrane.

3.5. Change of cell performance during humidity cycling

According to the variables to be controlled, there are several types of accelerated durability tests, for example, high-temperature operation, humidity cycle tests, Open-circuit voltage (OCV) tests, and freeze/thaw tests [25–28]. It is important to select test conditions that are suitable for the research objective; for example, an OCV durability test can be used to investigate chemical decomposition of the perfluorinated ionomer membrane by measuring the emission of fluoride ions [27]. In this study, a humidity cycle test was chosen to evaluate the effect of the composite membrane with improved dimensional stability on cell durability. For this test,
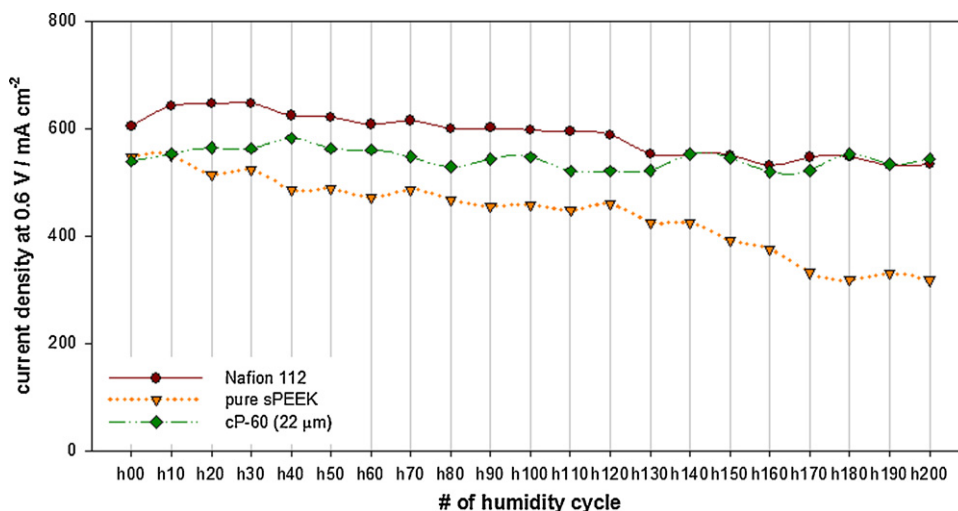
Fig. 7. Variations of current density with humidity cycling at 65 °C: response of current density is obtained at 0.6 V in current–voltage curves measured every 10 humidity cycles.

repeated hydration and dehydration was intensively imposed on three MEAs employing Nafion 112, pure sPEEK, and a thin cP-60 membrane. An H_2/air supply can cause chemical degradation, and thus it becomes difficult to distinguish the contribution from physical degradation by dimensional change from various other factors contributing to cell degradation behaviour. For this reason, nitrogen gas was supplied during the humidity cycle test.

The change in current density at 0.6 V in the current–voltage curves, measured every 10 humidity cycles, is presented in Fig. 7. The cell performance using the pure sPEEK membrane clearly decreases with humidity cycles and the current density after 200 humidity cycles is less than 60% of the initial value. The cell using a Nafion 112 membrane also suffers gradual degradation in performance after 100 humidity cycles, although the decay is less significant than that of a cell based on a pure sPEEK membrane. On the other hand, the current density of the cell based on the cP-60 membrane is stable over the entire humidity cycle period. Considering the significant degradation of the pure sPEEK membrane during humidity cycling, this improvement in performance stability of the cell based on the cP-60 membrane is quite remarkable. In the present experiment, all MEAs were assembled using the same components except for the membrane and the test conditions were tuned according to dimensional change by membrane swelling. Therefore, the difference in the performance stability of the cell during the humidity cycle test should be caused mainly by the dimensional stability of the membrane. This result is in good agreement with the prediction that the improved dimensional stability of the composite membrane would have a positive influence on the stability of the cell during the humidity cycle test.

4. Conclusions

A porous PVdF substrate has been prepared by extraction of a pore former, DPhP, and the porosity is controlled by the content of the pore former in the substrate. PVdF substrates with 60–80% of porosity are used to impregnate sPEEK electrolyte in order to provide good proton conduction. Compared with a Nafion membrane and a pure sPEEK membrane, the sPEEK/PVdF composite membrane exhibits a substantial reduction in water uptake and dimensional change, as well as an increase in mechanical strength under both dry and hydrated states. These improvements are attributed to suppressed hydration of the membranes, which results from the hydrophobic property of PVdF itself and the effect of the porous substrate as a mechanical support. A cell based on the composite membrane (cP-60) shows good stability during humidity cycle tests, whereas the cell performance using the pure sPEEK membrane showed significant degradation. The introduction of a porous PVdF substrate into a membrane is thus considered to be an efficient route for improving the dimensional stability of the membrane, which leads to enhanced stability of the cell during humidity cycling.

Acknowledgement

References

[1] A.F. Ghenciu, Curr. Opin. Solid State Mater. Sci. 6 (2002) 389.
[2] K.A. Mauritz, R.B. Moore, Chem. Rev. 104 (2004) 4535.
[3] K.D. Kreuer, J. Membr. Sci. 185 (2001) 29.
[4] M.A. Hickner, H. Ghassemi, Y.S. Kim, B.R. Einsla, J.E. McGrath, Chem. Rev. 104 (2004) 4587.
[5] Y. Yin, O. Yamada, K. Tanaka, K.-I. Okamoto, Polym. J. 38 (2006) 197.
[6] M. Sankir, Y.S. Kim, B.S. Pivovar, J.E. McGratha, J. Membr. Sci. 299 (2007) 8.
[7] Y.S. Kim, Advances in Materials for Proton Exchange Membrane Fuel Cell Systems 2007, CA, USA, 18–21 February, 2007.
[8] T. Yamaguchi, F. Miyata, S.-I. Nakaoa, J. Membr. Sci. 214 (2003) 283.
[9] T. Yamaguchi, H. Zhou, S. Nakazawa, N. Hara, Adv. Mater. 19 (2007) 592.
[10] X. Zhu, H. Zhang, Y. Liang, Y. Zhang, Q. Luo, C. Bi, B. Yi, J. Mater. Chem. 17 (2007) 386.
[11] T. Yamaguchi, H. Kuroki, F. Miyata, Electrochem. Commun. 7 (2005) 730.
[12] D.M. Xing, B.L. Yi, F.Q. Liu, Y.Z. Fu, H.M. Zhang, Fuel Cells 5 (2005) 406.
[13] L. Wang, B.L. Yi, H.M. Zhang, Y.H. Liu, D.M. Xing, Z.-G. Shao, Y.H. Cai, J. Power Sources 167 (2007) 47.
[14] L. Li, J. Zhang, Y. Wang, J. Membr. Sci. 226 (2003) 159.
[15] P. Xing, G.P. Robertson, M.D. Guiver, S.D. Mikhailenko, K. Wang, S. Kaliaguine, J. Membr. Sci. 229 (2004) 95.
[16] H. Strathmann, K. Kock, Desalination 21 (1977) 241.
[17] K. Kimmerle, H. Strathmann, Desalination 79 (1990) 283.
[18] K.-Y. Chun, S.-H. Jang, H.-S. Kim, Y.-W. Kim, H.-S. Han, Y.-I. Joe, J. Membr. Sci. 169 (2000) 197.
[19] H. Matsuyama, K. Nakagawa, T. Maki, M. Teramoto, J. Appl. Polym. Sci. 90 (2003) 292.
[20] V.R. Hande, S. Rao, S.K. Rath, A. Thakur, M. Patri, J. Membr. Sci. 322 (2008) 67.
[21] J. Hodakovska, J. Kleperis, L. Grinberga, G. Vaivars, Russ. J. Electrochem. 45 (2009) 657.
[22] K.A. Sung, H.-Y. Jung, W.-K. Kim, K.-Y. Cho, J.-K. Park, J. Power Sources 169 (2007) 271.
[23] E. Barsoukov, J.R. Macdonald, Impedance Spectroscopy: Theory, Experiment, and Applications, second ed., John Wiley & Sons, New York, 2005.

[24] R. O'Hayre, S.-W. Cha, W. Colella, F.B. Prinz, Fuel Cell Fundamentals, John Wiley & Sons, New York, 2006.
[25] D. Perti, Fuel Cell EXPO 2009, Tokyo, Japan, 25–27 February, 2009.
[26] S.D. Knights, K.M. Colbow, J. St-Pierre, D.P. Wilkinson, J. Power Sources 127 (2004) 127.
[27] M. Inaba, T. Kinumoto, M. Kiriake, R. Umebayashi, A. Tasaka, Z. Ogumi, Electrochim. Acta 51 (2006) 5746.
[28] A. Collier, H. Wang, X. ZiYuan, J. Zhang, D.P. Wilkinson, Int. J. Hydrogen Energy 31 (2006) 1838.